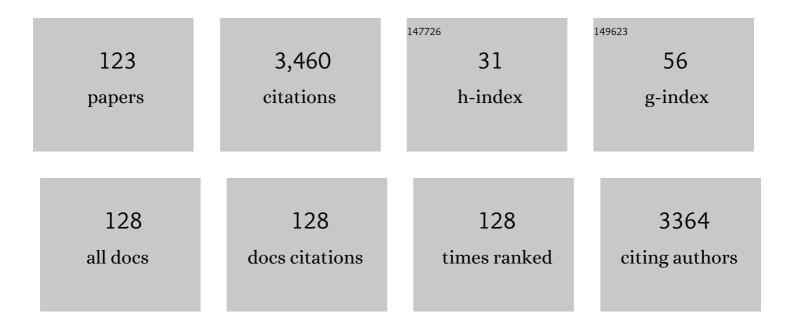
Herman L Offerhaus

List of Publications by Year in descending order

Source: https://exaly.com/author-pdf/8951196/publications.pdf Version: 2024-02-01



#	Article	IF	CITATIONS
1	Hexagonally Poled Lithium Niobate: A Two-Dimensional Nonlinear Photonic Crystal. Physical Review Letters, 2000, 84, 4345-4348.	2.9	468
2	Passively Q-switched 01-mJ fiber laser system at 153 ?m. Optics Letters, 1999, 24, 388.	1.7	225
3	High-energy, high-power ytterbium-doped Q-switched fiber laser. Optics Letters, 2000, 25, 37.	1.7	172
4	Raman microscopy for cellular investigations — From single cell imaging to drug carrier uptake visualization. Advanced Drug Delivery Reviews, 2015, 89, 71-90.	6.6	129
5	High-energy single-transverse-mode Q-switched fiber laser based on a multimode large-mode-area erbium-doped fiber. Optics Letters, 1998, 23, 1683.	1.7	124
6	Large Mode Area Fibers for High Power Applications. Optical Fiber Technology, 1999, 5, 185-196.	1.4	124
7	Characteristics of Q-switched cladding-pumped ytterbium-doped fiber lasers with different high-energy fiber designs. IEEE Journal of Quantum Electronics, 2001, 37, 199-206.	1.0	121
8	Chemical Imaging of Oral Solid Dosage Forms and Changes upon Dissolution Using Coherent Anti-Stokes Raman Scattering Microscopy. Analytical Chemistry, 2009, 81, 2085-2091.	3.2	89
9	Skin penetration behavior of lipid-core nanocapsules for simultaneous delivery of resveratrol and curcumin. European Journal of Pharmaceutical Sciences, 2015, 78, 204-213.	1.9	85
10	Label-Free Prostate Cancer Detection by Characterization of Extracellular Vesicles Using Raman Spectroscopy. Analytical Chemistry, 2018, 90, 11290-11296.	3.2	82
11	Classifying Raman spectra of extracellular vesicles based on convolutional neural networks for prostate cancer detection. Journal of Raman Spectroscopy, 2020, 51, 293-300.	1.2	79
12	Photoionization Microscopy. Physical Review Letters, 2002, 88, 133001.	2.9	77
13	A magnifying lens for velocity map imaging of electrons and ions. Review of Scientific Instruments, 2001, 72, 3245-3248.	0.6	68
14	Shot noise limited heterodyne detection of CARS signals. Optics Express, 2007, 15, 15207.	1.7	67
15	A route to sub-diffraction-limited â€ CARS Microscopy. Optics Express, 2009, 17, 22632.	1.7	63
16	Vibrational Phase Contrast Microscopy by Use of Coherent Anti-Stokes Raman Scattering. Physical Review Letters, 2009, 103, 043905.	2.9	63
17	Spatial alignment of diatomic molecules in intense laser fields: I. Experimental results. Journal of Physics B: Atomic, Molecular and Optical Physics, 2001, 34, 4919-4938.	0.6	59
18	Background free CARS imaging by phase sensitive heterodyne CARS. Optics Express, 2008, 16, 15863.	1.7	59

#	Article	IF	CITATIONS
19	25 kHz narrow spectral bandwidth of a wavelength tunable diode laser with a short waveguide-based external cavity. Laser Physics Letters, 2013, 10, 015804.	0.6	57
20	Application of a time-resolved event counting technique in velocity map imaging. Review of Scientific Instruments, 2002, 73, 4206-4213.	0.6	56
21	Pharmaceutical applications of non-linear imaging. International Journal of Pharmaceutics, 2011, 417, 163-172.	2.6	55
22	Passive Q-switching of fiber lasers using a broadband liquefying gallium mirror. Applied Physics Letters, 1999, 74, 3619-3621.	1.5	49
23	Creating Focused Plasmons by Noncollinear Phasematching on Functional Gratings. Nano Letters, 2005, 5, 2144-2148.	4.5	44
24	Noncritical phase-matched lithium triborate optical parametric oscillator for high resolution coherent anti-Stokes Raman scattering spectroscopy and microscopy. Applied Physics Letters, 2006, 89, 251116.	1.5	41
25	Spatially dependent Rabi oscillations: An approach to sub-diffraction-limited coherent anti-Stokes Raman-scattering microscopy. Physical Review A, 2010, 81, .	1.0	40
26	In situ dissolution analysis using coherent anti-Stokes Raman scattering (CARS) and hyperspectral CARS microscopy. European Journal of Pharmaceutics and Biopharmaceutics, 2013, 85, 1141-1147.	2.0	39
27	Axonâ€Myelin Unit Blistering as Early Event in <scp>MS</scp> Normal Appearing White Matter. Annals of Neurology, 2021, 89, 711-725.	2.8	39
28	High-gain waveguide amplifiers in Si ₃ N ₄ technology via double-layer monolithic integration. Photonics Research, 2020, 8, 1634.	3.4	36
29	Power scaling in passively mode-locked large-mode area fiber lasers. IEEE Photonics Technology Letters, 1998, 10, 1718-1720.	1.3	35
30	Application of spectral phase shaping to high resolution CARS spectroscopy. Optics Express, 2008, 16, 7985.	1.7	35
31	Ground-state depletion for subdiffraction-limited spatial resolution in coherent anti-Stokes Raman scattering microscopy. Physical Review A, 2012, 86, .	1.0	33
32	Wide wavelength-tuning of a double-clad Yb3+-doped fiber laser based on a fiber Bragg grating array. Laser Physics Letters, 2007, 4, 880-883.	0.6	32
33	Rapid identification of heterogeneous mixture components with hyperspectral coherent anti tokes Raman scattering imaging. Journal of Raman Spectroscopy, 2012, 43, 651-655.	1.2	32
34	Accurate and unbiased estimation of power-law exponents from single-emitter blinking data. Journal of Chemical Physics, 2006, 125, 204713.	1.2	31
35	Spatial alignment of diatomic molecules in intense laser fields: II. Numerical modelling. Journal of Physics B: Atomic, Molecular and Optical Physics, 2001, 34, 4939-4956.	0.6	26
36	COHERENT ANTI-STOKES RAMAN SCATTERING MICROSCOPY TO MONITOR DRUG DISSOLUTION IN DIFFERENT ORAL PHARMACEUTICAL TABLETS. Journal of Innovative Optical Health Sciences, 2009, 02, 37-43.	0.5	26

#	Article	IF	CITATIONS
37	Visualizing Resonances in the Complex Plane with Vibrational Phase Contrast Coherent Anti-Stokes Raman Scattering. Analytical Chemistry, 2010, 82, 7656-7659.	3.2	26
38	Stimulated-emission pumping enabling sub-diffraction-limited spatial resolution in coherent anti-Stokes Raman scattering microscopy. Physical Review A, 2013, 87, .	1.0	26
39	Parametric oscillator directly pumped by a 155-µm erbium-fiber laser. Optics Letters, 1999, 24, 975.	1.7	25
40	A theoretical investigation of superâ€resolution CARS imaging via coherent and incoherent saturation of transitions. Journal of Raman Spectroscopy, 2011, 42, 1854-1858.	1.2	25
41	Microfluidics control the ballistic energy of thermocavitation liquid jets for needle-free injections. Journal of Applied Physics, 2020, 127, .	1.1	24
42	Enhanced surface plasmon polariton propagation length using a buried metal grating. Journal of Applied Physics, 2011, 109, .	1.1	23
43	CARS microscopy as a tool for studying the distribution of micronised drugs in adhesive mixtures for inhalation. Journal of Raman Spectroscopy, 2014, 45, 495-500.	1.2	22
44	Large bandwidth, highly efficient optical gratings through high index materials. Optics Express, 2009, 17, 4268.	1.7	21
45	Phaseâ€shaping strategies for coherent antiâ€Stokes Raman scattering. Journal of Raman Spectroscopy, 2011, 42, 1859-1863.	1.2	20
46	Cancer-ID: Toward Identification of Cancer by Tumor-Derived Extracellular Vesicles in Blood. Frontiers in Oncology, 2020, 10, 608.	1.3	20
47	Coherent anti-Stokes Raman scattering microscopy driving the future of loaded mesoporous silica imaging. Acta Biomaterialia, 2014, 10, 4870-4877.	4.1	17
48	In-chip direct laser writing of a centimeter-scale acoustic micromixer. Journal of Micro/ Nanolithography, MEMS, and MOEMS, 2015, 14, 1.	1.0	17
49	Single-frequency operation of a broad-area laser diode by injection locking of a complex spatial mode via a double phase conjugate mirror. Optics Letters, 2006, 31, 1061.	1.7	16
50	Background-Free Nonlinear Microspectroscopy with Vibrational Molecular Interferometry. Physical Review Letters, 2011, 107, 253902.	2.9	15
51	All solid-state diode pumped Nd:YAG MOPA with stimulated Brillouin phase conjugate mirror. Optics Communications, 1996, 128, 61-65.	1.0	14
52	Chemically selective imaging by spectral phase shaping for broadband CARS around 3000 cm^â^'1. Journal of the Optical Society of America B: Optical Physics, 2009, 26, 559.	0.9	14
53	Polyglutamine Aggregate Structure In Vitro and In Vivo; New Avenues for Coherent Anti-Stokes Raman Scattering Microscopy. PLoS ONE, 2012, 7, e40536.	1.1	14
54	Near-field observation of spatial phase shifts associated with Goos-HÃ ¤ schen and Surface Plasmon Resonance effects. Optics Express, 2008, 16, 1958.	1.7	13

#	Article	IF	CITATIONS
55	Compact high-resolution spectral phase shaper. Review of Scientific Instruments, 2005, 76, 123105.	0.6	12
56	Exploring, tailoring, and traversing the solution landscape of a phase-shaped CARS process. Optics Express, 2010, 18, 2695.	1.7	12
57	Imaging local acoustic pressure in microchannels. Applied Optics, 2015, 54, 6482.	2.1	12
58	Highâ€resolution narrowband CARS spectroscopy in the spectral fingerprint region. Journal of Raman Spectroscopy, 2009, 40, 1229-1233.	1.2	11
59	Heterodyne interferometric polarization coherent antiâ€Stokes Raman scattering (HIPâ€CARS) spectroscopy. Journal of Raman Spectroscopy, 2010, 41, 1678-1681.	1.2	11
60	A hybrid semiconductor-glass waveguide laser. Proceedings of SPIE, 2014, , .	0.8	11
61	Comparison of three types of fiber optic sensors for temperature monitoring in a groundwater flow simulator. Sensors and Actuators A: Physical, 2021, 331, 112682.	2.0	11
62	Intracellular Delivery of Poorly Soluble Polyphenols: Elucidating the Interplay of Self-Assembling Nanocarriers and Human Chondrocytes. Analytical Chemistry, 2016, 88, 7014-7022.	3.2	10
63	Possibilities for Groundwater Flow Sensing with Fiber Bragg Grating Sensors. Sensors, 2019, 19, 1730.	2.1	10
64	Tethering Cells via Enzymatic Oxidative Crosslinking Enables Mechanotransduction in Nonâ€Cellâ€Adhesive Materials. Advanced Materials, 2021, 33, e2102660.	11.1	10
65	Hyperspectral imaging in biomedical applications. Journal of Optics (United Kingdom), 2019, 21, 010202.	1.0	9
66	Identification and quantification of 16 inorganic ions in water by Gaussian curve fitting of near-infrared difference absorbance spectra. Applied Optics, 2015, 54, 5937.	2.1	8
67	Single shot beam quality (M2) measurement using a spatial Fourier transform of the near field. Optics Communications, 1998, 151, 65-68.	1.0	6
68	Vibration transfers to measure the performance of vibration isolated platforms on site using background noise excitation. Review of Scientific Instruments, 2011, 82, 065111.	0.6	6
69	Shot noise limited heterodyne detection of CARS signals. , 2008, , .		5
70	Tailoring a coherent control solution landscape by linear transforms of spectral phase basis. Optics Express, 2010, 18, 973.	1.7	5
71	Coherent control of vibrational transitions: Discriminating molecules in mixtures. Faraday Discussions, 2011, 153, 227.	1.6	5
72	Phase aspects of (broadband) stimulated Raman scattering. Reviews in Analytical Chemistry, 2012, 31, 1-6.	1.5	5

#	Article	IF	CITATIONS
73	High precision wavelength estimation method for integrated optics. Optics Express, 2013, 21, 17042.	1.7	5
74	In plantaimaging of Δ9-tetrahydrocannabinolic acid inCannabis sativa L.with hyperspectral coherent anti-Stokes Raman scattering microscopy. Journal of Biomedical Optics, 2013, 18, 046009.	1.4	5
75	Q-factor measurements through injection locking of a semiconductor-glass hybrid laser with unknown intracavity losses. Optics Letters, 2014, 39, 1748.	1.7	5
76	Advances in nonlinear optical spectroscopies: a historical perspective of developments and applications presented at ECONOS. Journal of Raman Spectroscopy, 2016, 47, 1111-1123.	1.2	5
77	Micro-machining workstation for a diode pumped Nd:YAG high-brightness laser system. Review of Scientific Instruments, 1998, 69, 2118-2119.	0.6	4
78	Holographic injection locking of a broad area laser diode via a photorefractive thin-film device. Optics Express, 2007, 15, 17587.	1.7	4
79	73-nm tuning of a double-clad Yb3+-doped fiber laser based on a hybrid array. Laser Physics, 2008, 18, 353-356.	0.6	4
80	Dynamic Consolidation Measurements in a Well Field Using Fiber Bragg Grating Sensors. Sensors, 2019, 19, 4403.	2.1	4
81	Study on multiple waveguide platforms for waveguide integrated Raman spectroscopy. OSA Continuum, 2020, 3, 1322.	1.8	4
82	Fundamental mode intensity evolution in tapered optical fibres. Laser Physics, 2020, 30, 126204.	0.6	4
83	Modeling of mode locking in a laser with spatially separate gain media. Optics Express, 2010, 18, 22996.	1.7	3
84	Large scale scanning probe microscope: Making the shear-force scanning visible. American Journal of Physics, 2010, 78, 562-566.	0.3	3
85	Imaging of surface plasmon polariton interference using phase-sensitive photon scanning tunneling microscope. Applied Physics A: Materials Science and Processing, 2011, 103, 673-676.	1.1	3
86	Coherent anti-Stokes Raman Scattering (CARS) Microscopy Visualizes Pharmaceutical Tablets During Dissolution. Journal of Visualized Experiments, 2014, , .	0.2	3
87	Hybrid imaging of fluorescently labeled cancer drugs and label-free four-wave mixing microscopy of cancer cells and tissues. Journal of Biomedical Optics, 2015, 20, 086006.	1.4	3
88	Early interferometric detection of rolling contact fatigue induced micro-cracking in railheads. NDT and E International, 2017, 86, 14-19.	1.7	3
89	Numerical study of submicroparticle acoustophoresis using higher-order modes in a rectangular microchannel. Journal of Sound and Vibration, 2018, 415, 169-183.	2.1	3
90	The light-induced structural phase transition in confining gallium and its photonic applications. Journal of Luminescence, 2000, 87-89, 646-648.	1.5	2

#	Article	IF	CITATIONS
91	Non-reciprocal transmission via phase conjugation in multimode optical fibres. Optics Communications, 2001, 190, 357-365.	1.0	2
92	Vibrational phase contrast CARS microscopy for quantitative analysis. , 2010, , .		2
93	Design Considerations to Realize Differential Absorption-Based Optofluidic Sensors for Determination of Ionic Content in Water. IEEE Sensors Journal, 2018, 18, 6051-6058.	2.4	2
94	Nonlinear Optics Approaches Towards Subdiffraction Resolution in CARS Imaging. Neuromethods, 2014, , 291-324.	0.2	2
95	Nonlinear multispectral imaging for tumor delineation. Journal of Biomedical Optics, 2020, 25, .	1.4	2
96	Linear polarization Yb3+-doped fiber laser with novel innerclad structures. Laser Physics, 2008, 18, 1340-1343.	0.6	1
97	Background free CARS imaging by local phase detection. Proceedings of SPIE, 2009, , .	0.8	1
98	Laser induced damage reduction in single-mode fiber devices. Laser Physics, 2009, 19, 1030-1033.	0.6	1
99	Implementation of vibrational phase contrast coherent anti-Stokes Raman scattering microscopy. Applied Optics, 2011, 50, 1839.	2.1	1
100	Investigation of adaptive laser pulse shaping by direct estimation of group delay profile. Optics Communications, 2011, 284, 3748-3758.	1.0	1
101	Development and applications of nonlinear optical spectroscopy: 10th ECONOS/30th ECW meeting in Enschede, The Netherlands. Journal of Raman Spectroscopy, 2012, 43, 593-594.	1.2	1
102	Hyperspectral coherent anti-Stokes Raman scattering microscopy for in situ analysis of solid-state crystal polymorphs. Proceedings of SPIE, 2013, , .	0.8	1
103	Epi-detection of vibrational phase contrast coherent anti-Stokes Raman scattering. Optics Letters, 2014, 39, 5814.	1.7	1
104	Editorial for special issue on nano-optomechanics. Journal of Optics (United Kingdom), 2017, 19, 080401.	1.0	1
105	Role of temperature in de-mixing absorbance spectra composed of compound electrolyte solutions. Applied Optics, 2018, 57, 7871.	0.9	1
106	Optofluidic interferometry chip designs of differential NIR absorbance based sensors for identification and quantification of electrolytes. , 2016, , .		1
107	Thermal effects on tapered holmium-doped fiber amplifiers. Optical Engineering, 2020, 59, 1.	0.5	1
108	Diode-pumped 1-kHz high-power Nd:YAG laser with excellent beam quality. , 1997, 3092, 29.		0

#	Article	IF	CITATIONS
109	Engineered plasmon focusing on functional gratings. , 2005, 5840, 359.		0
110	Spectral phase shaping for high resolution CARS spectroscopy around 3000 cm-1. , 2009, , .		0
111	Dynamic Process Measurements in the Complex Plane with Vibrational Phase Contrast CARS. , 2010, , .		0
112	Vibrational Phase Contrast CARS Imaging. , 2010, , .		0
113	A common path interferometer for stimulated Raman scattering (SRS) and coherent anti-Stokes Raman scattering measurements (CARS). Proceedings of SPIE, 2012, , .	0.8	0
114	Computational optimization of phase shaped CARS. Proceedings of SPIE, 2012, , .	0.8	0
115	Background-free nonlinear microspectroscopy with vibrational molecular interferometry. , 2012, , .		0
116	<i>In situ</i> dissolution analysis of pharmaceutical dosage forms using coherent anti-Stokes Raman scattering (CARS) microscopy. Proceedings of SPIE, 2014, , .	0.8	0
117	A First Step towards Determining the Ionic Content in Water with an Integrated Optofluidic Chip Based on Near-Infrared Absorption Spectroscopy. Optics, 2020, 1, 175-190.	0.6	0
118	Temperature and Consolidation Sensing Near Drinking Water Wells Using Fiber Bragg Grating Sensors. Water (Switzerland), 2020, 12, 3572.	1.2	0
119	Femtosecond spectral phase shaping for CARS spectroscopy and imaging. Springer Series in Chemical Physics, 2009, , 523-525.	0.2	0
120	Single polarization Yb. , 2011, , .		0
121	Sub-diffraction-limited spatial resolution in CARS microscopy by ground state depletion. , 2012, , .		0
122	Stimulated Emission Pumping Enabling Sub-Diffraction-Limited Spatial Resolution in CARS Microscopy. , 2012, , .		0
123	Analysis and modeling of CLBG using the transfer matrix method. , 2019, , .		0